



3-2-3

## A PROPOSAL FOR ESTIMATION OF SOURCE TIME FUNCTION BASED ON STRONG GROUND MOTIONS

Yoshikazu KITAGAWA<sup>1</sup> and Takahito INOUE<sup>2</sup>

<sup>1</sup>Head of IISEE, Building Research Institute, Ministry of Construction,  
Tsukuba-shi, Ibaraki, Japan

<sup>2</sup>Research Engineer, Technical Research Institute, HAZAMA-GUMI, LTD.,  
Yono-shi, Saitama, Japan

### SUMMARY

In this paper, we propose a analytical method for estimating the source time function by applying the autoregressive (AR) model to the observed ground motions. This method is applied to the ground motions synthesized by the fault model. As a result, the source time function obtained by using this method corresponds to the moment rate function and the same conditions are obtained as those given for the fault model analysis. Further, we apply this method to the observed strong ground motions during the 1983 Nihonkai-Chubu Earthquake (M=7.7). The source time function and the locations of two major events agree with those obtained by the Inversion Method.

### INTRODUCTION

In order to use the synthetic seismograms calculated from the fault model as input motion for earthquake resistant design of structures, it is necessary to estimate the source characteristics from the observed ground motions correctly. However, the ground motions are affected by the earthquake process itself, the propagating path of the seismic wave, the topography of the ground surface, and the properties of ground surface layers. The Inversion Method proposed by Kikuchi et al. (Ref.1) is one method by which the source characteristics can be estimated. In this method, the parameters for the fault and the distribution of events on the fault plane are determined by matching the synthetic waveforms with the observed ones.

In this paper, we propose the analytical method for estimating the source time function from the observed ground motions by using the autoregressive (AR) model for the purpose of estimating the dynamic properties of the ground surface and the seismic wave path. In order to verify this method, we apply this procedure to the ground motions synthesized by the fault model (Ref.2). Further, this analytical method is applied to the observed strong ground motions during the 1983 Nihonkai-Chubu Earthquake (M=7.7) and the results are compared with those obtained by the Inversion Method.

### ANALYTICAL METHOD

Estimation of Source Time Function In order to estimate the dynamic properties of the ground surface and the seismic wave path, we apply the AR model to the tail part of the observed ground motion which appears as the finite discrete time

series,  $X_i$  ( $i=1,2,\dots,N$ ). As the tail part,  $tX_i$  ( $i=L,L+1,\dots,N; l \leq L \leq N$ ), is random data with few non-stationary properties, it is written as

$$tX_i = \sum_{m=1}^M A_m X_{i-m} + F_i \quad ; \quad i=L,L+1,\dots,N \quad (1)$$

where  $A_m$  ( $m=1,2,\dots,M$ ) is the AR coefficient for minimizing the average square error,  $M$  is the AR order and  $F_i$  is the error series. Then, in order to determine the suitability of a given AR model, Akaike's final prediction error (FPE) (Ref.3) is introduced. Upon using the AR coefficient obtained by Eq.(1),  $A_m$ , the estimated value from the observed ground motion,  $eX_i$  is represented by the following equation as the linear combination with former values.

$$eX_i = \sum_{m=1}^M A_m X_{i-m} \quad ; \quad i=M,M+1,\dots,N \quad (2)$$

As the values shown in Eq.(2) include the dynamic properties of the observation site, the residual time series defined by Eq.(3),  $E_i$  includes much data related to the source characteristics.

$$E_i = X_i - eX_i = X_i - \sum_{m=1}^M A_m X_{i-m} \quad ; \quad i=M,M+1,\dots,N \quad (3)$$

Upon separating the non-stationary property from the residual time series shown in Eq.(3), the finite discrete time series expressed in Eq.(4),  $rE_i$  is obtained.

$$rE_i = W_i sE_i \quad ; \quad i=M,M+1,\dots,N \quad (4)$$

where  $sE_i$  is the finite discrete time series with the stationary gaussian process and  $W_i$  is the weight function which gives the non-stationary properties to the amplitude. Further, by integrating the finite discrete time series obtained from Eq.(4),  $sE_i$ , it becomes possible to estimate the source time function.

$$\dot{M}_i = \alpha \int sE_i dt \quad ; \quad i=M,M+1,\dots,N \quad (5)$$

where  $\alpha$  is the coefficient including the soil constants at the fault.

Distribution of Events in the Fault Plane When the observed ground motions include the multiple shock sequence, it is necessary to decide the time difference between events, the seismic moment and the distribution of the individual events in the fault plane. We assume that a homogeneous half space with a constant S-wave velocity of  $V_e$  exists and the relationship among events and observation points, as shown in Fig.1. Then, the time difference at the  $k$ -th observation point,  $T_{jk}'$  can be obtained as a function of  $T_j$ ,  $L_j$ ,  $\theta_j$ ,  $\phi_j$ ,  $V_e$  and the coordinates of the  $k$ -th observation point in the coordinate system shown in Fig.1 (Ref.4). Where  $T_j$  and  $L_j$  are the time difference of the origin times and the distance between the first and  $j$ -th events respectively, and  $\theta_j$  and  $\phi_j$  are the azimuths of the  $j$ -th event from the first event. The unknown parameters ( $T_j$ ,  $L_j$ ,  $\theta_j$ ,  $\phi_j$ ) can be determined by minimizing the sum of the squared residuals, i.e.,

$$\sum_{k=1}^N (T_{jk}'' - T_{jk}')^2 = \min \quad (6)$$

where  $N$  is the total number of observation points,  $T_{jk}''$  is the observed time difference between the first and the  $j$ -th events.

Further, the area under each wave pack on the source time function expressed in Eq.(5) gives the seismic moment of the individual event. We estimate the height of the peak,  $M_j$  and the duration time,  $\tau_j$  by assuming that the sum of the seismic moment of each event satisfies the following relation.

$$0.9 M_0 \leq \sum_{j=1}^J M_j \tau_j \leq 1.1 M_0 \quad (7)$$

where  $J$  is the total number of events and  $M_0$  is the total seismic moment of the

earthquake obtained by the relationship,  $\log M_0 = 1.5 M + 16$  (Ref.5), and M is the magnitude of the earthquake.

## NUMERICAL ANALYSIS

Analytical Model and Its Characteristics In order to verify this analytical method, this procedure is applied to the ground motion synthesized by using the estimation method developed by Kitagawa et al. (Ref.6). The used underground structure and the fault parameters are shown in Fig.2 and Table 1, respectively. The relation between the fault and the observation point(OP-1) is shown in Fig.7 and the epicentral distance is 113km. The synthesized velocity seismograms with one event, which has the source time function shown in Fig.5 as a dotted line, are shown in Fig.3. This numerical analysis is mainly concerned with the body wave.

When the AR model is applied to the tail part of the observed ground motion, it is necessary to select the appropriate AR order and the appropriate time length of the tail part of the observed ground motion. In this analysis, we follow the criterion for application of the AR model proposed in Ref.7. As a result, Fig.4 shows the coherence between the waveform obtained from residuals in Eq.(3) and the incident waves at point A and B. The waveform obtained from the residuals agrees with the incident wave at point A and it is suggested that the finite discrete time series including the source characteristics is separated from the observed ground motion.

Property of Distribution of Events The source time function obtained from Eq.(5) is shown in Fig.5 as a solid line and corresponds to the moment rate function. We can identify the earthquake with a single event. The seismic moment estimated from the area under the source time function is  $0.66 \times 10^{26}$  dyn-cm. This result agrees with the given condition for the fault model analysis, shown in Fig.5 as a dotted line.

Fig. 6 shows the results for when this procedure is applied to the synthesized ground motion with the multiple events. The source time function consists of two wave packs with the distinct peak and shows the earthquake as two events. The second peak is smaller than the first and the seismic moment of the second event is underestimated more than the given condition for analysis, but the total seismic moment is  $0.68 \times 10^{26}$  dyn-cm. The time difference between the two events is longer than the given condition for analysis because of the Doppler effect. Further, Fig.7 shows the relative location and the time difference between the two events obtained by using the results at three observation points. These results agree with the condition used in the fault model analysis of Table 1.

## APPLICATION TO OBSERVED GROUND MOTIONS

Estimation of Source Time Function We apply this analytical method to the strong ground motions recorded at four observation points listed in Table 2 during the 1983 Nihonkai-Chubu Earthquake ( $M=7.7$ ). Three-component accelerograms were recorded at each observation point. In order to standardize the radiation pattern, we use the major principal axis component of the observed ground motion in the horizontal plane (Ref.8). As an example, Fig.8(a) shows the velocity seismogram at Aomori (AOM) used in the present analysis. Further, the waveform obtained from the residuals and the source time function as a result of applying this procedure to the observed ground motion are shown in Fig.8(b), (c), respectively. Judging from these figures, we identify two major events as marked in Fig.8(c).

Relationship between Two Major Events Since no absolute times are marked on the

records, we shall locate the second event relative to the first event by using the time difference between the two events on the source time function. Table 2 summarizes the time differences between the two events. We determine that  $T=27s$ ,  $L=35km$ ,  $\Theta=20^\circ$  assuming  $V_e=3.5km/s$  and  $\phi=0^\circ$ . These epicenters are shown in Fig.9 together with four observation points used in this study. We also assume that the location of the first event is the main-shock epicenter determined by the Japan Meteorological Agency (JMA). Further, we estimate that the seismic moments of the first and second events are  $1.87$  and  $1.55 \times 10^{27}$  dyn-cm, respectively. The results obtained by the Inversion Method (Ref.9) are shown in Fig.8(c) and Fig.9, where the radius of the circle shown in Fig.9 denotes the estimated seismic moment. From these figures, the source time function and the relative locations of the two major events agree with those obtained by the Inversion Method.

#### CONCLUSIONS

In this paper, the analytical method is proposed for estimating the source time function by applying the autoregressive (AR) model to the observed ground motions. The results of application to the ground motions synthesized by the fault model analysis shows the usefulness of this method in estimating the source time function, the seismic moment of the individual event and their distribution on the fault plane. Further, this method is applied to the observed strong ground motions during the 1983 Nihonkai-Chubu Earthquake. The source time function and the relative locations of the two major events agree with those obtained by the Inversion Method. It is pointed that this analytical method can estimate the source time function of the seismic moment from the observed ground motions.

#### ACKNOWLEDGEMENTS

We would like to thank Mr. Toshihide KASHIMA and Mrs. Yukie HAGISHIMA of IISEE, Building Research Institute, Ministry of Construction, Japan for kindly offering much help.

#### REFERENCES

1. Kikuchi, M., Kanamori, H., "Inversion of complex body waves," Bull. Seism. Soc. Am., Vol.72, pp.491-506, 1982.
2. Kitagawa, Y., Inoue, T., "Study on source time function of strong ground motion (in Japanese with English summary)," Proc. of 7th JEES., pp.157-162, 1986.
3. Akaike, H., "Fitting autoregressive models for prediction," Ann. Inst. Statist. Math., Vol.21, pp.243-247, 1969.
4. Sato, T., "Rupture characteristics of the 1983 Nihonkai-Chubu (Japan Sea) Earthquake as inferred from strong motion accelerograms," J. Phys. Earth, 33, pp.525-557, 1985.
5. Kasahara, K., "Standard values of fault parameters (in Japanese)," Program and Abstracts of the Seismological Society of Japan, No.2, p.8, 1975.
6. Kitagawa, Y., Sudo, K., Yoshimura, N., "Strong motion estimation due to a realistic earthquake faulting," Proc. of Pacific Conf. Earthq. Eng., 1978.
7. Inoue, T., Kitagawa, Y., Nishide, T., "Estimation method on characteristics of source function (part 3) (in Japanese)," Summaries of Technical Papers of Annual Meeting of A.I.J., Vol.B, 1988.
8. Penzien, J., Watabe, M., "Characteristics of 3-dimensional earthquake ground motions," Earthquake Eng. Struct. Dynamics, Vol.3, pp.365-373, 1975.
9. Ishikawa, Y., Takeo, M., Hamada, N. et al., "Source process of the 1983 Japan Sea earthquake (in Japanese)," Chikyū, 6, pp.11-17, 1984.

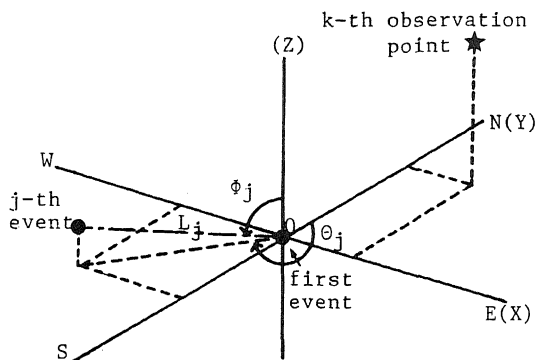


Fig. 1 Geometric relation among events and observation points

observation point	layer thickness $H$ (km)	P-wave velocity $V_p$ (km/s)	S-wave velocity $V_s$ (km/s)	density $\rho$ ( $t/m^3$ )
surface layers	0.012	0.56	0.17	1.5
	0.03	1.26	0.38	2.0
	0.208	1.34	0.55	2.0
basement	0.75	1.71	0.70	2.0
body wave	1.2	3.0	1.3	2.1
* source	2.8	4.4	2.0	2.4
	$\infty$	6.6	3.54	2.7

Fig. 2 Model of underground structure

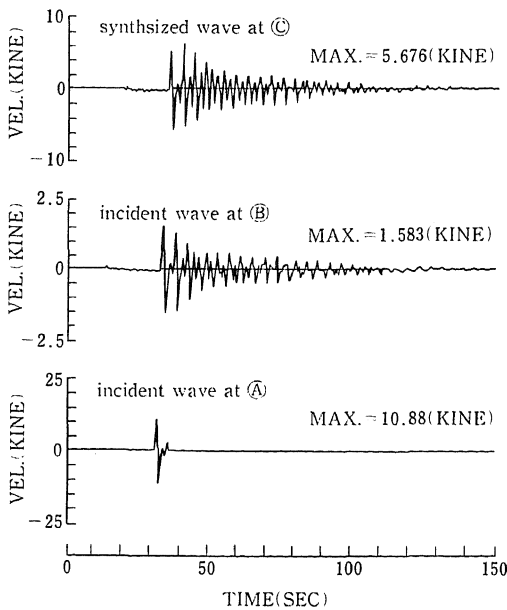


Fig. 3 Synthesized ground motions with one event

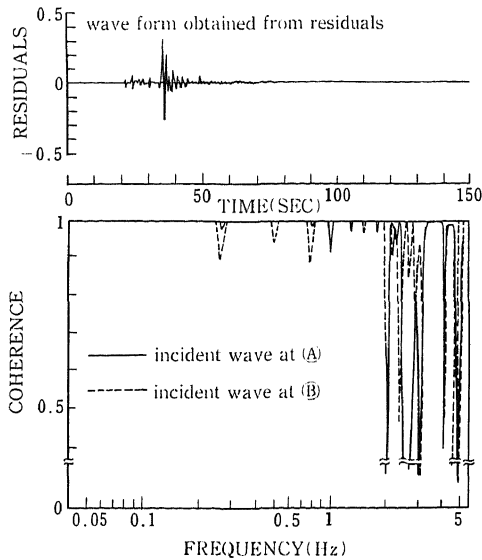


Fig. 4 Coherence between waveform obtained from residuals and incident waves

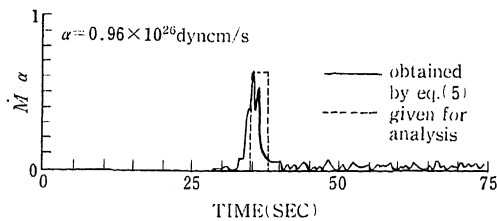


Fig. 5 Source time function

Table 1 Fault parameters

seismic moment ( $M_0$ )	$1.0 \times 10^{26}$ (dyn-cm)
forcal depth (D)	8 (km)
dip angle ( $\delta$ )	100 (deg)
slip angle ( $\lambda$ )	170 (deg)
dislocation ( $D_0$ )	100 (cm)
strike ( $\phi$ )	N80° W
rise time ( $\tau$ )	1.0 (sec)
fault length (L)	20 (km)
fault width (W)	10 (km)
rupture velocity ( $V_r$ )	3.0 (km/s)

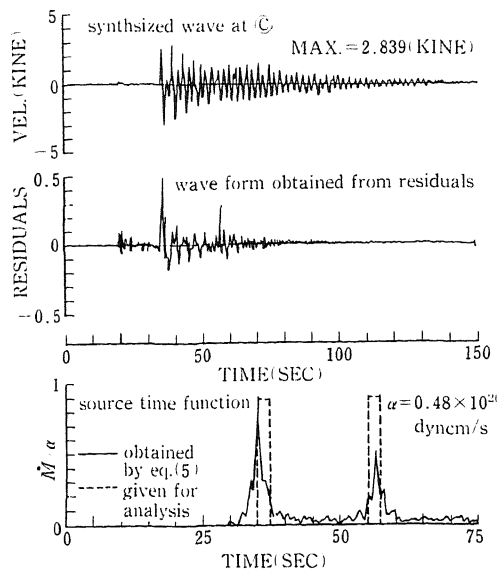


Fig. 6 Analytical results in the case of synthesized ground motion with two events

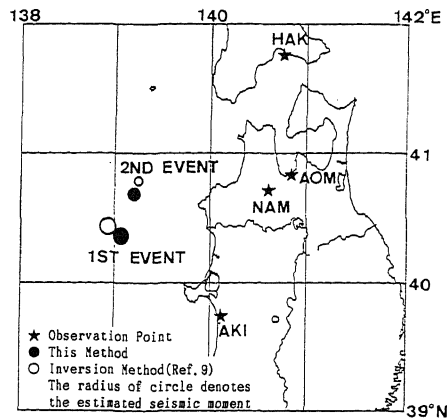


Fig. 9 Relative locations of the first and the second major events and observation points

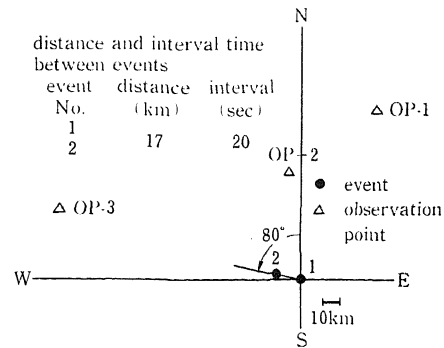


Fig. 7 Locations of events and observation points

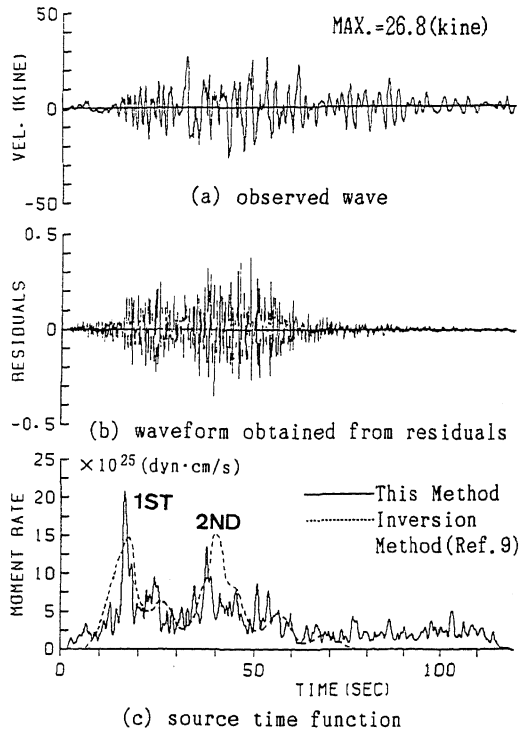


Fig. 8 Analytical results in the case of observed ground motion at Aomori

Table 2 Observation point in the present study

Station Name	Station Code	Distance (km)	T" (s)	Operating Institution
AKITA	AKI	114	17.7	PHRI*
AOMORI	AOM	157	21.0	PHRI*
NAMIOKA	NAM	137	22.7	TAAB**
HAKODATE	HAK	210	30.8	PHRI*

Epicentral distances are calculated for the epicenter of the main-shock determined by JMA, T" is the time difference between two major events, \*PHRI:Port and Harbour Research Institute, \*\*TAAB:Tohoku Agricultural Administration Bureau.